Accepted Manuscript

Intraperitoneal injection of microencapsulated Sertoli cells restores muscle morphology and performance in dystrophic mice

Sara Chiappalupi, Giovanni Luca, Francesca Mancuso, Luca Madaro, Francesca Fallarino, Carmine Nicoletti, Mario Calvitti, Iva Arato, Giulia Falabella, Laura Salvadori, Antonio Di Meo, Antonello Bufalari, Stefano Giovagnoli, Riccardo Calafiore, Rosario Donato, Guglielmo Sorci

PII: S0142-9612(15)00833-9

DOI: 10.1016/j.biomaterials.2015.10.029

Reference: JBMT 17126

To appear in: *Biomaterials*

Received Date: 14 June 2015

Revised Date: 30 September 2015

Accepted Date: 14 October 2015

Please cite this article as: Chiappalupi S, Luca G, Mancuso F, Madaro L, Fallarino F, Nicoletti C, Calvitti M, Arato I, Falabella G, Salvadori L, Di Meo A, Bufalari A, Giovagnoli S, Calafiore R, Donato R, Sorci G, Intraperitoneal injection of microencapsulated Sertoli cells restores muscle morphology and performance in dystrophic mice, *Biomaterials* (2015), doi: 10.1016/j.biomaterials.2015.10.029.

Intraperitoneal injection of microencapsulated Sertoli cells restores muscle morphology and performance in dystrophic mice

Sara Chiappalupi[1,8,*], Giovanni Luca[1,*], Francesca Mancuso[1], Luca Madaro[3,4,8], Francesca Fallarino[1], Carmine Nicoletti[5,8], Mario Calvitti[1], Iva Arato[1], Giulia Falabella[1], Laura Salvadori[1], Antonio Di Meo[6], Antonello Bufalari[6], Stefano Giovagnoli[7], Riccardo Calafiore[2,§], Rosario Donato[1,8,§], and Guglielmo Sorci[1,8,§]

[1]Department of Experimental Medicine, University of Perugia, Perugia 06132, Italy; [2]Department of Medicine, University of Perugia, Perugia, Italy; [3]IRCCS Fondazione Santa Lucia, Rome 00143, Italy; [4]National Research Council, Institute of Cell Biology and Neurobiology, Fondazione Santa Lucia, Rome 00143, Italy; [5]Unit of Histology, DAHFMO, La Sapienza University, Rome 00161, Italy; [6]Department of Veterinary Medicine, University of Perugia, Perugia 06126, Italy; [7]Department of Pharmaceutical Sciences, University of Perugia, Perugia 06123, Italy; [8]Interuniversity Institute of Myology (IIM)

* Equally contributed to the present work

§ Share senior authorship of this paper

Correspondence should be addressed to G.S.

Running title

Sertoli cells restore dystrophic muscle function

Abstract

Duchenne muscular dystrophy (DMD) is a genetic disease characterized by progressive muscle degeneration leading to impaired locomotion, respiratory failure and premature death. In DMD patients, inflammatory events secondary to dystrophin mutation play a major role in the progression of the pathology. Sertoli cells (SeC) have been largely used to protect xenogeneic engraftments or induce trophic effects thanks to their ability to secrete trophic, antiinflammatory, and immunomodulatory factors. Here we have purified SeC from specific pathogen-free (SPF)-certified neonatal pigs, and embedded them into clinical grade alginate microcapsules. We show that a single intraperitoneal injection of microencapsulated SPF SeC (SeC-MC) in an experimental model of DMD can rescue muscle morphology and performance in the absence of pharmacologic immunosuppressive treatments. Once i.p. injected, SeC-MC act as a drug delivery system that modulates the inflammatory response in muscle tissue, and upregulates the expression of the dystrophin paralogue, utrophin in muscles through systemic release of heregulin-β1, thus promoting sarcolemma stability. Analyses performed five months after single injection show high biocompatibility and long-term efficacy of SeC-MC. Our results might open new avenues for the treatment of patients with DMD and related diseases.

MAIN TEXT

Introduction

Duchenne muscular dystrophy (DMD) is a lethal, recessive X-linked disease with an incidence of 1 in 3600 live male births caused by the absence of dystrophin following mutation of *DMD* gene [1,2]. Since dystrophin is involved in the structural stabilization of the sarcolemma, DMD patients

experience membrane fragility of the myofibers which results in persistent degeneration/regeneration cycles causing progressive depletion of the muscle stem cell pool, and replacement of the skeletal muscle contractile components with fibrous and adipose tissue. The progressive muscle weakness leads to impaired locomotion in childhood, confinement to a wheelchair by 12 years of age, and premature death because of respiratory and/or cardiac failure [1,2]. Persistent compensative degenerative/regenerative cycles and the consequent chronic inflammation in muscle tissue are recognized as major factors in the outcome of DMD pathology [3,4]. DMD patients are currently being treated with antiinflammatory steroids, which are the only evidence-based effective treatment for these patients so far, albeit with limited efficacy and undesired side effects [5-7].

Sertoli cells (SeC), a major component of the seminiferous tubules, are long known for their ability to secrete trophic, antiinflammatory, and immunomodulatory factors. In the testis SeC are responsible for a unique immune-privileged environment that protects developing germ cells from the host's immune system attack [8,9]. Because of their properties, SeC have been largely used to protect co-grafted allogeneic and xenogeneic tissues from the immune destruction in several settings [10,11]. Also, SeC induced trophic effects on neurons in experimental models of Parkinson's disease and amyotrophic lateral sclerosis, and showed beneficial antiinflammatory effects when grafted into an experimental model of Huntington's disease [12-14]. In the recent past we improved the use of SeC by encapsulating them in highly purified sodium alginate microcapsules [15]. Intraperitoneal injection of microencapsulated SeC resulted in a TGF-β-dependent restoration of systemic immune tolerance, diabetes prevention and reversion in spontaneous diabetic NOD mice [16], and promoted IGF-1-mediated body growth in a murine model of Laron syndrome (dwarfism) [17]. Here we have further improved SeC-based technology by isolating SeC from testes of specific pathogen-free (SPF)-certified neonatal pigs, obtaining pure, viable and functional SeC, and encapsulating them into clinical grade alginate-based microcapsules (SeC-MC) meeting the requirements of National Formulary and European Pharmacopoeia.

We show that intraperitoneal (i.p.) injection with SPF SeC-MC in acute-phase dystrophic *mdx* mice results in a dramatic reduction of infiltrating inflammatory cells, fibrotic areas, and necrotic myofibers in muscle tissue, and acquisition of resistance to exercise-induced muscle damage. SeC-MC restrain muscle inflammation by promoting the enrichment in antiinflammatory macrophages in the muscle mononuclear cell population, and upregulate utrophin at the sarcolemma of myofibers thus mimicking the function of dystrophin, through systemic delivery of heregulin β1. Notably, a single injection of SeC-MC remarkably reduces necrosis and fibrosis in the diaphragm (i.e., the chronically damaged muscle in *mdx* mice) in long-term analysis, and exerts beneficial effects in chronic-phase and presymptomatic dystrophic mice.

Results

Purified SPF SeC show high viability and functionality after encapsulation

SeC isolated and purified from testes of SPF-certified Large White neonatal pigs were composed of ~97% anti-Müllerian hormone-positive (Sertoli) cells [18], ~1.5% alpha-smooth muscle actin-positive (peritubular myoid) cells, ~1.0% insulin-like 3-positive (Leydig) cells, and ~0.5% protein gene product 9.5-positive (gonocytes and spermatogonial) cells, as assessed by FACS and immunofluorescence analysis (Fig. 1, A and B). Freshly purified SPF SeC were encapsulated using a newly-composed microdroplet generator in highly biocompatible, clinical grade (endotoxin levels ≤0.5 EU/g) alginate-based microcapsules. The obtained microcapsules were elastic and translucent, morphologically homogeneous with round shape and no tails or coalescence (Fig. 1C). The microcapsules were fairly monodispersed, with an extremely narrow size distribution (mean diameter, 600±45 μm). Importantly, the current procedure permitted to increase the number of encapsulated cells from $1.0x10^7$ [15,19] to $2.0x10^7$ SeC/ml alginate. SeC viability and functionality proved unaffected by the encapsulation procedure since i) ethidium bromide/fluorescein diacetate

double staining showed that ~96-97% SeC were viable before or after encapsulation (Fig. 1D), and ii) measurement of α-aromatase activity revealed similar levels of 17-β-estradiol production before and after encapsulation, in both the absence or presence of FSH (Fig. 1E).

SeC-MC treatment improves muscle morphology in *mdx* mice

We injected microencapsulated SPF SeC (SeC-MC; equivalent amount to $1.0x10^6$ SeC per gram of body weight) or the same amount of empty microcapsules (E-MC) into the peritoneal cavity of 4-week-old *mdx* mice, i.e., dystrophic mice in the acute phase of the pathology [20]. Three weeks after injection, compared with muscles of mock-treated mice, the muscles of SeC-MC-treated mice showed reduced mononuclear cell infiltrate, and hallmarks of efficient muscle regeneration, that is a dramatic reduction of necrotic myofibers, a reduced percentage of regenerating (small and centrally-nucleated) myofibers, and increased percentages of regenerated (normally-sized and centrally-nucleated) and undamaged (normally-sized and with peripheral nuclei) myofibers (Fig. 2, A and B; Supplementary Fig. 1A). Accordingly, the frequency histograms of single-fiber area in TA muscles from SeC-MC-treated *vs* mock-treated mice showed a shift toward higher values (2641.28 *vs* 1894.62 μm^2 average cross-sectional area [CSA], respectively) which were more similar to those of untreated age-matched WT controls (average CSA, 2825.13 μm^2) (Fig. 2C), further pointing to the establishment of a microenvironment suitable for efficient regeneration. This was also evidenced by the marked reduction of the numbers of $PAX7^+$ cells (i.e., quiescent satellite cells/proliferating myoblasts), $MyoD^+$ cells (activated satellite cells/proliferating myoblasts), and $myogenin^+$ cells (differentiating myoblasts/myocytes) in TA, *Gastrocnemius* (GC) and diaphragm (DIA) muscles of SeC-MC-treated *vs* mock-treated mice (Supplementary Fig. 2).

Moreover, immunohistochemical analysis of the activated macrophage marker, MAC3, showed a dramatic reduction of the areas infiltrated with macrophages in the muscles of SeC-MC-treated *mdx* mice compared with mice injected with E-MC (Fig. 2, D and E; Supplementary Fig. 1B) pointing to a local antiinflammatory effect exerted by the intraperitoneally located SeC. Finally, *mdx* mice

treated with SeC-MC showed a dramatic reduction of muscle fibrosis (Fig. 2, F and G; Supplementary Fig. 1C). This latter result appears relevant as fibrosis is a major issue in DMD patients; fibrous and adipose tissues progressively overtake the functional myofibers thus concurring to a progressive muscle wasting. Notably, DIA, the most affected muscle in *mdx* model [21], showed ~82% reduction of fat deposition following treatment with SeC-MC compared with DIA of *mdx* mice treated with E-MC (Supplementary Fig. 1D).

SeC-MC treatment rescues muscle performance in *mdx* mice

The overall morphological improvement observed in muscles of dystrophic mice after i.p. injection of SeC-MC translated into recovery of muscle performance, as assessed by treadmill running tests. SeC-MC-treated *mdx* mice stopped fewer times (4.5±0.45 *vs* 9.5±0.98 stops for SeC-MC- and mock-treated *mdx* mice, respectively, in a 30-min run) (Fig. 3A), and ran longer distances for longer times compared with the mock-treated counterpart (Fig. 3B), similar to untreated WT mice. Noteworthy, SeC-MC-treated *mdx* mice acquired resistance to exercise-induced muscle damage, since Evans blue dye (EBD) infiltration tests at the end of the exercise protocol revealed a marked reduction of the number of damaged myofibers in *Quadriceps femoris* (QF) muscles of SeC-MC- *vs* mock-treated *mdx* mice, which could be appreciated even at macroscopic inspection (Fig. 3, C and D).

The antiinflammatory effect of SeC-MC treatment is an early event

Looking for a molecular mechanism underpinning the rapid recovery of muscle homeostasis in SeC-MC-treated dystrophic mice, we further investigated the antiinflammatory effects of i.p.-injected SeC on muscle tissue. Already one week after injection muscles of SeC-MC-treated *mdx* mice had reduced $MAC3^+$ areas and MAC3 levels (71.2% and 62% reduction, respectively) compared with mock-treated mice three weeks after injection (Fig. 4, A and B). At 1 week post-injection, the mononuclear cell infiltrate (mainly composed of macrophages) isolated from hind

limb muscles of SeC-MC-treated animals showed a significant reduction of expression of inflammatory cytokines, including interleukin (IL)-6, IL-12 p35, IL-12 p40 and interferon (IFN)-γ, and upregulation of the antiinflammatory cytokine, IL-10 (Fig. 4C) known to induce in dystrophic muscles a shift of macrophages from a cytolytic/M1 to a tissue-repairing/M2 phenotype [22]. Transforming growth factor (TGF)-β, which has a major role in the antiinflammatory effects induced by SeC in several experimental settings [16,23], and a key role in mediating fibrosis in muscle tissue [24], resulted slightly but significantly downregulated in the mononuclear cell infiltrate isolated from muscles of SeC-MC-treated *mdx* mice (Fig. 4C). In line with the expression levels of the tested cytokines, the mononuclear cells from muscles of SeC-MC-treated *mdx* mice expressed smaller amounts of inducible nitric oxide synthase (*Nos2*) and larger amounts of arginase 1 (*Arg1*) transcripts, markers of proinflammatory and antiinflammatory macrophages [25], respectively, compared with mock-treated *mdx* mice (Fig. 4D). Thus, treatment of dystrophic animals with SeC-MC might favor the transition of the muscle macrophage population towards an antiinflammatory/reparative (M2) phenotype. In support, *Cd163* and *Mrc1* (CD206), which are markers of M2 macrophages, resulted overexpressed in lympho-mononuclear cell infiltrate isolated from hind limb muscles of SeC-MC-treated compared with mock-treated *mdx* mice (Fig. 4E).

SeC-MC treatment upregulates utrophin in *mdx* mice

Next, we analyzed muscles for the expression of utrophin, a dystrophin autosomal paralogue whose overexpression prevents muscle damage in dystrophic mice [26]. One week after injection muscles of SeC-MC-treated *mdx* mice showed induction of *Utrn* expression (Fig. 5A) resulting in 2.8-fold increase in utrophin levels compared with mock-treated mice (Fig. 5B). In SeC-MC-treated *mdx* mice utrophin was homogeneously localized to the myofiber periphery, i.e. to the sarcolemma (Fig. 5C), a condition necessary for utrophin to efficiently replace the function of dystrophin and prevent sarcolemma damage [27]. This is because at the sarcolemma utrophin is able to recruit a utrophin-associated protein complex (UAPC) which shares many components with the dystrophin-associated

protein complex (DAPC) [2,28]. Notably, we found that SeC-MC treatment resulted in the appearance at the myofiber periphery of α- and β-dystroglycan, and β1- and β2-syntrophin (Supplementary Fig. 3), which are components of both DAPC and UAPC, thus further supporting a functional replacement of dystrophin with SeC-induced utrophin in our conditions.

Heregulin β1 is a neuregulin-1 type I polypeptide that transactivates the utrophin A promoter via ERK-dependent activation of the *ets*-related transcription factor complex GABPα/β in cultured muscle cells [29,30]. Heregulin β1 has been reported to ameliorate the dystrophic phenotype through the upregulation of utrophin expression when i.p. injected in *mdx* mice [31]. Purified porcine SeC express an mRNA predictably encoding heregulin β1 (Supplementary Fig. 4, A and B) and proteins recognized by an anti-(human)heregulin β1 antibody with similar molecular weights as in U87 cells (as a positive control) (Supplementary Fig. 4C). Encapsulated porcine SeC release heregulin β1 in the culture medium *in vitro* (Fig. 5D), demonstrating that encapsulation does not hamper the diffusion of the protein towards the external milieu. When co-cultured with SeC-MC, myotubes obtained from C2C12 or primary *mdx* myoblasts showed high utrophin and activated ERK1/2 levels (Supplementary Fig. 5, A-C), and these effects were almost completely abolished upon addition to the culture medium of an anti-heregulin β1 antibody or the MEK1/ERK1/2 inhibitor, PD98059 (Supplementary Fig. 5, A-D). TGFβ, which can activate ERK1/2 through a non-canonical pathway [32] resulted not involved in the upregulation of utrophin (Supplementary Fig. 5E). We also found that i) one week after i.p. injection heregulin β1 serum levels were ten times higher in SeC-MC-treated *mdx* mice compared with controls (Fig. 5E), and ii) SeC-MC failed to upregulate utrophin and rescue muscle morphology when i.p. injected along with a heregulin β1 blocking antibody (Fig. 5, F-I). In this latter condition we detected even smaller muscle utrophin levels than in mock-treated *mdx* mice (Fig. 5F). Concomitantly, muscles from SeC-MC-treated mice injected with anti-heregulin β1 antibody showed intermediate (3.21±0.31%) percentages of necrotic myofibers between those detected in non-immune IgG-injected SeC-MC-treated mice and

those detected in IgG-injected mock-treated mice (Fig. 5, G and H). Also, anti-heregulin β1 antibody treatment of SeC-MC-treated mice did not significantly affect the area of macrophage infiltration in *mdx* muscles compared with their internal controls, with areas of macrophage infiltration being restricted to damaged myofibers in both cases (Fig. 5, G and I). In accordance, western blot analysis revealed similar amounts of MAC3 between SeC-MC-treated mice injected with either anti-heregulin β1 antibody or non-immune IgG (Fig. 5F). This suggested that i.p. injected SeC-MC independently i) release heregulin β1 thereby promoting utrophin induction in myofibers and sarcolemma stability and reducing damage-induced macrophage infiltration, and ii) secrete immunomodulatory factors that concur to reduce inflammation.

SeC-MC treatment is effective in chronic *mdx* mice

Next, we evaluated the efficacy of i.p. injection of SeC-MC in chronic dystrophic mice. 12-month-old *mdx* mice reproduce chronic DMD conditions since their muscles (especially the DIA) are characterized by accumulation of fibrous and adipose tissue, a hallmark of progressive degeneration [33]. Three weeks after injection, SeC-MC significantly reduced adipose and fibrous tissue deposition in muscles (Figure 1, A, B, D, G and I in Ref. [34]). Macrophage infiltrate and muscle damage were reduced in chronic *mdx* mice treated with SeC-MC, as investigated by MAC3 immunohistochemistry in DIA and TA (Figure 1, C, D, H and I in Ref. [34]), and autofluorescence analysis of the QF after EBD injection (Figure 1E in Ref. [34]). Finally, compared with muscles of mock-treated *mdx* mice muscles of SeC-MC-treated mice showed upregulated utrophin (2.7-fold increase in protein amount) (Figure 1J in Ref. [34]), which was localized to the periphery of the myofibers (Figure 1K in Ref. [34]). Similar results as above were obtained after treatment of dystrophic animals during the pre-symptomatic phase. Indeed, 2-week-old *mdx* mice, which show only minor signs of muscle degeneration (94.4±6.1% undamaged myofibers in TA muscles) (Figure 2A in Ref. [34]) resulted protected against the necrosis of myofibers and muscle inflammation by the i.p. injection of SeC-MC as evidenced by histological and immunohistochemical analyses

performed three weeks after injection (Figure 2, A and B in Ref. [34]), when utrophin expression resulted about five-fold increased and properly localized (Figure 2, C and D in Ref. [34]). However, we did not observe full prevention suggesting that pathogenic mechanisms leading to muscle degeneration and subsequent activation of regeneration cycles are already active in *mdx* mice at the age of two weeks, as evidenced by histological analysis of the percentages of centrally-nucleated myofibers in SeC-MC-treated mice at the beginning and the end of the treatment (Figure 2A in Ref. [34]).

SeC-MC preserve muscle architecture in long-term treatments

We next explored long-term effects of SeC-MC in dystrophic animals. To address this point, we treated 4-week-old *mdx* mice with a single i.p. injection of SeC-MC or E-MC and performed analyses five months later. Noteworthy, five months after injection both empty and SeC-containing microcapsules were found freely floating in the peritoneal cavity, morphologically intact and devoid of fibrotic tissue overgrowth (Fig. 6, A and B'), with high retention of embodied cell viability (68.32±2.9% mean viability) (Fig. 6C), highlighting their high biocompatibility and potential use in long-term treatments (also see 18). Compared with control DIA, DIA of SeC-MC-treated mice showed reduced EBD infiltration (Fig. 6, D-F), fat deposition (Fig. 6, G, H and O), fibrotic areas (Fig. 6, I, J and O), and $MAC3^{+}$ areas (Fig. 6k,l,o). Utrophin was still present at the periphery of the myofibers (Fig. 6, M and N).

Discussion

DMD gene is the largest human gene (2.4 Mb) made of 79 exons which account for 0.6% of its total sequence. About 4,700 different mutations have been reported in the *DMD* gene, and about 90% of patients with a mutation that disrupts the open reading frame of the *DMD* gene develop the DMD

phenotype, which is characterized by progressive reduction of muscle performance and premature death [1,2]. Despite huge efforts to find a cure, antiinflammatory steroids represents the current standard treatment for DMD patients. This is because inflammatory events secondary to *DMD* mutation play a major role in the progression of the pathology [3,4], and the therapeutic approaches to DMD proposed so far have revealed intrinsic limitations and/or require pharmacological immunosuppression (as for cell-based or viral vector-centered therapies), so that combinatorial approaches are encouraged [5].

Microencapsulation provides a useful means to confine cells in a specific space, avoiding their uncontrolled dispersion inside the host's body in case of engraftment. At the same time, microencapsulation provides a special 3D microenvironment that greatly helps spatial distribution of the enveloped cells, resulting in retention of cell viability and functionality, while preserving the ability of encapsulated cells to release their own factors and sense the host's ones [35]. Also, microencapsulation protects enveloped cells from the host's immune system attack, which is particularly important in the case of cell types unable to modulate the immune response [36,37]. Injected microencapsulated cells can be easily retrieved by peritoneal lavage thereby circumventing another major regulatory obstacle that would be inevitably encountered by using naked cells. Pigs represent an ideal source of transplantable cells in terms of reproducibility and safety since pigs can be bred under strictly controlled, specific pathogen-free conditions, and permit to overcome several limits linked to the use of nonhuman primates, including the risk to transmit retroviruses potentially infectious for humans, ethical concerns and breeding costs [38].

SeC secrete numerous trophic and immunomodulatory factors required for the orderly development and immunoprotection of maturing germ cells that otherwise would be recognized by the host's immune system [8,9]. This ability of SeC prompted investigators to use them in a large number of experimental settings to give trophic support or immunomodulate the host's immune reaction, especially in case of allo- or xenogeneic engraftment [9-11]. The use of SeC has been recently improved by their encapsulation into biocompatible materials [16,17].

Here we have set up a unique method to isolate SeC from SPF neonatal pigs and encapsulate them into highly biocompatible, clinical grade alginate-based microcapsules. We report that SPF porcine SeC-MC act as a "micro-biofactory" and drug delivery system able to improve muscle morphology and performance by secreting immunomodulatory and trophic factors [8,9,11] once injected into the peritoneal cavity of dystrophic mice. After i.p. injection of SeC-MC we found an improvement of muscle architecture in acute-, chronic-phase, and presymptomatic dystrophic mice, suggesting that the cocktail of factors secreted by SeC-MC are beneficial to dystrophic muscle tissue in the different phases of the pathology. Among the hallmarks of SeC-MC treatment in *mdx* mice are a reduction of the percentages of necrotic myofibers and regenerating myofibers in favor of regenerated and undamaged myofibers (Fig. 2, and Supplementary Fig. 1), and a reduction of the number of activated muscle precursor cells (Supplementary Fig. 2) compared with control mice. This reflects the establishment of a microenvironment that supports an efficient regeneration of damaged myofibers and prevents further muscle damage. The observed beneficial effects of SeC-MC treatment are mainly linked to the release by SeC of immunomodulatory factors and factor(s) capable of upregulating utrophin. This translates into a rapid (Figs. 4, A and B, and 5, G and I) and dramatic (Figs. 2, D and E, 4, A and B, and 6, K, L and O, Supplementary Fig. 1B, and Figs.1, H and I, and 2B in Ref. [34]) reduction of activated macrophages and the upregulation of utrophin in myofibers in SeC-MC-treated muscles in the experimental conditions tested. The reduction of infiltrating macrophages following injection of SeC-MC is associated with reduced expression of proinflammatory cytokines in dystrophic muscles (Fig. 4C) and a shift of muscle macrophages towards an antiinflammatory (arginase 1^{+}) phenotype (Fig. 4D) known to have a key role in tissue reconstructive processes [26,39]. While the antiinflammatory action of SeC contributes to preserve muscle morphology by reducing the damage induced by proinflammatory macrophages, the upregulation of utrophin compensates for dystrophin lack thus reducing the myofiber necrosis following contraction and further limiting the inflammatory response. The expression of the dystrophin paralogue, utrophin is developmentally regulated in healthy muscle tissue, utrophin

being diffusely expressed along the entire sarcolemma in the post-natal phase and confined to the myotendineous and neuromuscular junctions in adulthood [40,41]. However, re-expression of utrophin at the sarcolemma occurs after muscle damage in regenerating myofibers [42]. Since utrophin is able to recruit at the sarcolemma a similar protein complex to DAPC, namely UAPC [2,28], utrophin overexpression is investigated as a potential therapeutic approach to DMD [6,43]. We found that in muscles of dystrophic mice treated with SeC-MC utrophin amounts increased up to 4.8 fold compared to control mice (Fig. 5, B and F, and Figs. 1J and 2C in Ref. [34]), and utrophin is localized to the sarcolemma together with members of the UAPC/DAPC, which might have a relevant role in protecting muscle morphology. Noteworthy, a two- or threefold increase in utrophin levels has been shown to be sufficient to ameliorate the dystrophic phenotype in *mdx* mice [44].

While the antiinflammatory effects exerted by SeC is the result of the combined action of multiple factors [8,9,11] which are difficult to dissect, we identified heregulin β1 secreted by the intraperitoneally located SeC-MC as a major inducer of utrophin at muscle level in our experimental settings (Fig. 5, F and G). Interestingly, heregulin but neither EGF, PDGF, IGF-1 nor IGF-2 resulted the most efficacious factor in inducing utrophin mRNA in C2C12 myotubes [29]. However, IGF1, which is known to sustain muscle hypertrophy and to be secreted by SeC [17], might have a role in the increased CSA observed in SeC-MC-treated animals (Fig. 2C). Whether SeC also accelerate the myogenic differentiation process remains to be investigated.

Antiinflammatory effects and utrophin upregulation appear to be distinct effects of SeC; indeed, *in vivo* blockade of heregulin β1 dampens the recovery of muscle morphology, thus potentially stimulating macrophage infiltration, but this latter is simultaneously reduced by SeC-derived immunomodulatory factors (Fig. 5, G-I). This multimodal activity of SeC represents an important advantage over the administration of antiinflammatory drugs or induction of utrophin expression as obtained by heregulin β1 injection, which resulted in only marginal improvements when administered after 30 days from birth [45].

A single i.p. injection of SeC-MC into acute-phase *mdx* mice protects DIA from degeneration and fibrosis in long-term analysis. The microcapsules result biologically invisible to the host immune system, and show high retention of embodied cell viability, which represents an additional advantage in case of employment of the present procedure for long-term treatments.

The proposed protocol is endowed with translational potential since i) non-encapsulated SeC have been successfully co-transplanted with porcine islets of Langerhans in type-1 diabetic patients in order to immunoprotect pancreatic islets from rejection, without associated complications in a 7-years follow-up [46,47]; ii) we used encapsulated and SPF porcine SeC, which confer substantial safety on the procedure; and, iii) it does not involve any pharmacologic immunosuppression. While further experimentation in higher mammals is needed, we envision the use of SPF porcine SeC-MC as a pioneering therapeutic approach that might open new avenues for treatment of DMD and related myopathies.

Materials and Methods

Isolation and characterization of Sertoli cells

SeC were isolated from SPF-certified pre-pubertal (7-20 day-old) Large White pig testes. Pigs were grown in a unique SPF herd (Experimental Zooprophylactic Institute of Lombardia and Emilia Romagna, Brescia, Italy), hauled in sterile boxes and transported to the surgical suite (Department of Veterinary, University of Perugia) where they underwent bilateral orchidectomy after general anesthesia [40 mg/kg ketamine (Ketavet, Intervet, Italy) and 40 μg/kg dexmedetomidine (Dexdomitor, Orion Corporation, Finland)]. After removal under anesthesia, the testes were finely chopped to obtain a homogeneous tissue that underwent enzymatic digestion with collagenase P (2 mg/ml; Roche Diagnostics, Italy) for 20 min at 37°C in Hanks' balanced salt solution (HBSS) followed by digestion with trypsin and DNase I (Sigma-Aldrich, USA) for 10 min at 37°C [17]. The

pellet was passed through a 500-µm stainless steel mesh and resuspended in glycine to eliminate residual Leydig and peritubular cells [48]. The resulting SeC were cultured in HAM's F-12 (Euroclone, Italy) supplemented with retinoic acid (0.166 nM; Sigma-Aldrich) and insulin-transferrin-selenium (ITS, Becton Dickinson) (1:100) in 5% CO_2 at 37°C. After 3 days of culture, SeC were incubated with 10 mM tris-hydroxymethyl-aminomethane hydrochloride (TRIS; Sigma-Aldrich) buffer to eliminate residual germ cells [49]. SeC were characterized by immunofluorescence and FACS analysis for AMH, INSL3, ASMA and PGP9.5. In immunofluorescence the percentages of positive cells were determined by three independent operators. In FACS analysis an isotype antibody followed by labelled secondary antibody was used as a control. Yield was ~$1.5x10^8$ SeC/pig. SeC viability was assessed by staining with ethidium bromide/fluorescein diacetate (both from Sigma-Aldrich). Viable cells were evaluated by counting at least 10 randomly chosen fields at a 20x magnification by three independent operators. SeC functional activity was evaluated by measuring α-aromatase activity [15]. For α-aromatase activity, 1.0×10^6 SeC were treated for 3 days with 1 mg/ml of FSH (Serono, Italy), thereafter exposed to 0.2 mg/ml of testosterone enanthate (SIT, Italy) for 8h. At the end of the incubation period, the supernatant was used to determine 17-β-estradiol concentration by direct chemiluminescence (ADVIA Centaur, Estradiol-6 III, Bayer Diagnostics, Germany) (intra-assay CV<4.0%; interassay CV=6.0%).

Microencapsulation of Sertoli cells

Sodium alginate meeting National Formulary and European Pharmacopoeia requirements (Keltone® LVCR; FMC BioPolymer, PA, USA) was added to saline to obtain 1.6-2.0% (w/v) alginate solution (viscosity 120-150 mPa.s), and the pH was adjusted to 7.4-7.6. This gave structurally unmodified salts of alginate with a mannuronate/guluronate (M/G) ratio of 1.093, and endotoxin content lower than 0.5 EU/g. Freshly-prepared (passage zero) SeC were enveloped in barium alginate microcapsules (SeC-MC) using a microdroplet generator. Only preparations with

greater than 90% SeC and greater than 90% viable cells (see above) were employed for encapsulation. Briefly, confluent monolayers of SeC were collected after incubation with 0.05% trypsin/EDTA, washed twice, counted by hemocytometer and suspended in 1.6% aqueous solution of sodium alginate. The cell suspension was continuously mixed by means of a magnetic stirrer to prevent cell aggregation and obtain a homogeneous distribution of SeC within the alginate solution. The cell suspension was continuously aspirated by a peristaltic pump (flow rate, 14 ml/min) and thereafter extruded through a microdroplet generator (air flow rate, 1.5-2 l/min) under sterile conditions. The microdroplet generator includes an air-jet device where the combination of air flow and mechanical pressure, made the suspension sprayed in form of microdroplets. The distance from nozzle tip to surface of gelling bath was 42 mm. The obtained microdroplets were ionically cross-linked by collecting them on a $BaCl_2$ solution (1.2% w/v) which immediately turned them into gel microbeads with entrapped SeC. Indeed, as a divalent cation barium displaces sodium from alginate thus creating Ba-alginate beads that are water insoluble. The obtained microcapsules containing SeC (SeC-MC) were washed twice in saline, and cultured in HAM's F-12 (Euroclone, Italy) supplemented with retinoic acid (0.166 nM) and ITS (1:100) in 5% CO_2 at 37°C for 1 hour to eliminate barium excess. Viability of encapsulated SeC was evaluated by ethidium bromide/fluorescein diacetate staining as above. Viable cells (means±SEM) were evaluated by counting at least thirty randomly chosen microcapsules at magnification 20x by three independent operators using Scion Image 4.0.3.2 software. Micro-particle morphology, size and size distribution were assessed using inverted phase microscope and stereomicroscope by analyzing at least 300 particles/batch. The level of barium released from SeC-MC was determined over time by Inductively Coupled Plasma - Optical Emission Spectrometry (ICP-OES) using a Varian 700-Es series spectrometer (Agilent, Italy). Results showed that no release of barium occurs from SeC-MC up to 40 hours of culture (data not shown).

Animals

In vivo studies were performed on 2-week-, 4-week- or 12-month-old male *mdx* mice (C57BL/10ScSn-*Dmd*^{mdx}/J, original breeding from Jackson Laboratory) raised on a 12h light/day cycle and a standard mouse diet. SeC-MC or E-MC were injected into the peritoneal cavity of recipient mice by a sterile 16-gauge catheter under general anesthesia. We transplanted $1.0x10^6$ SeC/g body weight at a concentration of $1.0x10^7$ SeC/ml in saline (NaCl 0.9%). The procedures and experiments on mice were approved by the Ethics Committee of the Perugia University and the Italian Ministry of Health. No adverse effects of i.p. injection of SeC-MC or E-MC could be noticed during the entire course of the experimentation.

Cell culture

C2C12 myoblast cell line and primary myoblasts isolated from *mdx* mice [50] were cultured in high-glucose Dulbecco's modified Eagle's medium (HG-DMEM) supplemented with 20% fetal bovine serum (Invitrogen, USA), 100 U/ml penicillin, and 100 mg/ml streptomycin (growth medium, GM). Cells were maintained in a humidified atmosphere containing 5% CO_2 at 37°C. Confluent cells were shifted to differentiation medium [DM, HG-DMEM supplemented with 2% horse serum (HS, Invitrogen) and penicillin/streptomycin] to induce myogenic differentiation (i.e., myotube formation). Myotubes obtained from C2C12 or primary *mdx* myoblasts were further co-cultured for 24-48h with SeC-MC ($4.0x10^5$ SeC/ml) or the same amounts of E-MC, using 0.4 µm transwells (BD Biosciences) in the absence or presence of a heregulin β1 neutralizing antibody (ProSci, USA; cat. 38-254; 2 µg/ml), a TGF-β neutralizing antibody (clone 1D11; R&D Systems, cat. MAB1835; 20 µg/ml) or the same amount of non-immune IgG. Where indicated, cells were pre-treated with the MEK/ERK1/2 pathway inhibitor, PD98059 (Sigma-Aldrich; 20 µM in DMSO). Control cells received the same amounts of DMSO. Lympho-mononuclear cells were isolated [22] from hind limb muscles of 4-week-old male *mdx* mice one week after i.p. injection with SeC-MC (n=10) or E-MC (n=10). Muscles were dissected, cleaned of discernible non-muscle tissue, and rinsed with cold PBS before being chopped and treated with collagenase type IV (Sigma-Aldrich) in

HBSS (10 mg/ml). After incubation at 37°C for 45 min, the suspension was aspirated, centrifuged at 850g and resuspended in HBSS. The cell suspension was filtered through a 70-µm cell strainer, centrifuged at 850g, resuspended in HBSS, counted and applied to 15 ml of Histopaque 1077 (Sigma-Aldrich). After centrifugation at 1000g for 30 min, the cells at the Histopaque/HBSS interface were collected, centrifuged again, resuspended in PBS and counted. Same amounts of cells from SeC-MC- and E-MC-treated mice were processed for further real-time PCR analysis.

Morphological analyses

Muscles were isolated, formalin-fixed and paraffin-embedded in order to maximally preserve morphology. Muscle cross-sections measuring 4 µm were obtained and processed for standard haematoxylin/eosin (H&E) or Mallory staining. Quantifications on muscle sections were performed by three independent operators blinded to treatments. Sections at 100 µm intervals for each muscle were analyzed. The entire area of each section was evaluated to avoid bias. Areas with sectioning artifacts (folds, tears, etc.) were avoided. After H&E staining, the percentages of undamaged, regenerating, regenerated, and necrotic myofibers per section were manually counted by three independent operators according to the following parameters [51]: i) undamaged fibers, identified by the presence of peripheral nuclei; ii) regenerated fibers, identified by normal size but with central nuclei; iii) regenerating fibers, identified by small size, basophilic cytoplasm and central nuclei; and, iv) necrotic fibers, identified by pale cytoplasm and phagocytosis. Areas of fat deposition were identified by the evacuated spaces generated by the histochemical delipidation. Myofiber cross-sectional area (CSA) and the percentages of fibrotic areas (*blue*, after Mallory staining) were measured using Scion Image 4.0.3.2 software (NIH, Bethesda, USA). Slices were analyzed and photographed with a bright field microscope (Olympus BX51) equipped with a digital camera. Values reported are given as mean (±SEM) obtained from multiple animals as specified in each figure. For the evaluation of myofiber necrosis mice were i.p. injected with a 1% Evan's Blue Dye (EBD) solution (Sigma-Aldrich) at 1% volume relative to body mass 16-24h prior to tissue

sampling. Muscles were isolated and flash frozen in a pre-cooled beaker of isopentane placed in liquid nitrogen. Cryosections were fixed in acetone at -20°C. An anti-laminin antibody (Sigma-Aldrich, L9393; 1:50) followed by an AlexaFluor 488-conjugated anti-rabbit IgG (Invitrogen, 1:100) was used to mark individual myofibers. Nuclei were counterstained with 4',6-diamidino-2-phenylindole (DAPI; Sigma-Aldrich). Negative controls (not shown) bypassed the primary antibody treatment. The samples were analyzed by an epifluorescence microscope (Leica DMRB) equipped with a digital camera.

Immunohistochemistry and immunofluorescence

Paraffin sections of muscles were cut at 4 µm, deparaffinized with xylene and rehydrated in a graded ethanol series. Antigen retrieval was obtained by boiling for 1.5h in 10 mM citric acid buffer (pH 6.0), and depletion of endogenous peroxidase was accomplished by treatment with 3% H_2O_2. Sections were washed with TBS, pH 7.4, incubated for 1h with blocking buffer [BB; TBS containing 0.01% Tween-20 (T-TBS) and 10% HS] and probed with the following antibodies (1:50 in BB): anti-PAX7 (R&D Systems, USA; cat. MAB1675), and anti-MyoD (clone 5.8A; sc32578) and anti-myogenin (clone F5D; sc12732) (both from Santa Cruz Biotechnology, USA). After overnight incubation at 4°C, the sections were incubated with the appropriate biotinylated secondary antibody (Vector Laboratories, USA, 1:500) for 1h in BB. The sections were rinsed with T-TBS, and incubated for 45 min with Vectastain ABC reagents (Vector Laboratories). In the case of MAC3 detection, an anti-MAC3 antibody (clone M3/84; BD Biosciences, USA, cat. 553322) was used followed by incubation with horseradish peroxidase (HRP)-conjugated anti-rat IgG antibody (Santa Cruz Biotechnology, 1:500). Sections were incubated with 0.01% 3,3-diaminobenzidine tetrahydrochloride (DAB), and 0.006% H_2O_2 in 50 mM Tris-HCl, pH 7.4. Nuclei were counterstained with haematoxylin. The slices were then dehydrated, mounted with EuKitt mounting medium (Electron Microscopy Sciences, USA), and analyzed and photographed with a bright field microscope (Olympus BX51) equipped with a digital camera. Immunofluorescence

reactions on tissue slices were performed as above except that PBS, pH 7.4, and a different BB (i.e., 0.4% Triton-X-100, 10% donkey serum and 1% BSA in PBS) were used. The following primary antibodies were used: anti-α-dystroglycan (H-300, sc28534; 1:50), anti-β-dystroglycan (F-15, sc26539; 1:50), anti-β1-syntrophin (C-20, sc13763; 1:50), anti-β2-syntrophin (C-17, sc13766; 1:50), and mouse monoclonal anti-utrophin (clone 8A4; sc33700; 1:20) antibodies (all from Santa Cruz Biotechnology). TRITC-conjugated anti-mouse or anti-goat IgG antibodies (all from Sigma-Aldrich; 1:50) were used as secondary antibodies. Where indicated, acetone-fixed cryosections (7 µm) were used to detect utrophin using the same primary and secondary antibodies as above diluted in 1% BSA in PBS. Nuclei were counterstained with DAPI. After rinsing, samples were mounted with fluorescent mounting medium (Dako Corporation, Denmark) and viewed in an epifluorescence microscope (Leica DMRB) equipped with a digital camera. Immunostaining for AMH, INSL3, ASMA and PGP9.5 were performed as follows (16). SeC monolayers were grown on glass chamber slides and fixed in 4% paraformaldehyde (PFA) in PBS for 30 min. Fixed cells were permeabilized (PBS, 0.2% Triton X-100) for 10 min at room temperature and blocked with 0.5% BSA (Sigma-Aldrich) in PBS for 1h prior to exposure to polyclonal goat anti-AMH (C-20, Santa Cruz Biotechnology, sc6886; 1:100), polyclonal rabbit anti-INSL3 (Novus Biologicals, NBP1-18706; 1:200), polyclonal rabbit anti-ASMA (Abcam, ab5694; 1:200) or monoclonal rabbit anti-PGP9.5 (Abcam, ab108986; 1:200) antibody overnight at 4°C. The cells were then washed three times for 5 min in PBS and exposed to the secondary Alexa 488-conjugated donkey anti-goat or anti-rabbit antibody (both from Molecular Probes; 1:500). The cells were treated with RNAse (10 mg/ml; Sigma-Aldrich) and counterstained with DAPI. Negative controls (not shown) bypassed the primary antibody treatment. Cells were mounted on slides with ProLong® Gold antifade reagent (Molecular Probes). The percentages of AMH-, INSL3-, ASMA- and PGP9.5-positive cells were determined by using an epifluorescence microscope (BX-41; Olympus) equipped with a digital camera (F-viewer, Olympus). Images were processed with Cell F imaging software (Olympus) and ten different fields were counted by two independent operators blinded to treatments.

Western blotting

Muscle tissue was homogenized in 10 mM Tris, pH 7.4, 2.5% v/v sodium dodecyl sulfate (SDS), 100 mM dithiothreitol (DTT), in the presence of a mixture of protease inhibitors (Sigma-Aldrich). SeC, U87 and C2C12 cells, and primary *mdx* myoblasts were also lysed in the buffer above. The amount of protein in each sample was determined by Bradford assay, and equal amounts of protein were size-separated by SDS-PAGE. The following primary antibodies were used: anti-utrophin (clone 8A4; Santa Cruz Biotechnology, 1:500); anti-MAC3 (clone M3/84; BD Biosciences, 1:1000); anti-heregulin β1 (ProSci, cat. 38-254; 1:1000); anti-phospho-ERK1/2 (Thr202/Thr204) (Cell Signaling Technology, USA, cat. 9101; 1:1000); and, anti-ERK1/2 (cat. M5670; 1:10000), anti-α-actinin (cat. A7811; 1:1000), and anti-α-tubulin (clone DM1A, cat. T9026; 1:10000) (all from Sigma-Aldrich). After incubation with the appropriate HRP-conjugated secondary antibodies, the immune reaction was developed by enhanced chemiluminescence (SuperSignal West Femto Maximum or SuperSignal West Pico, both from Thermo Scientific, USA).

Reverse transcription-PCR and real-time PCR

Total RNA from SeC and U87 cells (a human glioblastoma cell line used as a positive control for the expression of heregulin β1) were extracted by the TRIzol reagent (Life Technologies) according to the manufacturer's instructions and reverse-transcribed with M-MLV Reverse Transcriptase (Life Technologies) prior to PCR analysis. The following primer pairs were used in PCR (28 cycles: denaturation at 95°C for 30 sec, annealing at 60°C for 30 sec, and extension at 72°C for 30 sec) to amplify human and porcine HRG-beta1 transcripts: 5'-ACTGGGACAAGCCATCTTGT-3' and 5'-GAGGGGTTTGAAAGGTCT-3' (98bp); 5'-ACTGGGACAAGCCATCTTGT-3' and 5'-TTGTTTCGTTCAGACCGAAG-3' (335bp); 5'-AAATCGCCCCCTTCGGAAAT-3' and 5'-CAATAGGGTCTTGGTTAGC-3' (580bp). β-actin (*Actb*, 5'-TCTGGCACCACACCTTCT-3' and 5'-TGATCTGGGTCATCTTCTCAC-3') was used as an internal control. After amplification, the

samples were electrophoresed on a 1.2-1.5% agarose gel, and the amplification products were revealed by ethidium bromide staining. Total RNA from hind limb skeletal muscles or lympho-mononuclear cells isolated from hind limb muscles (see Cell Culture procedures above) were extracted by the TRIzol reagent and reverse-transcribed as above. Real-time PCR analyses of mRNA contents were performed on Stratagene Mx3000P (Agilent Technologies, USA) by using HOT FIREPol EvaGreen qPCR Mix Plus (ROX) ready-to-use solution (Solis BioDyne, Estonia) in the presence of the following primers: *Utrn*, 5'-CCAGTGAGCATATTGTTGAGAG-3' and 5'-GCCTCCTGTGCCATTAAGAC-3'; *Il1b*, 5'-TGACGTTCCCATTAGACAACTG-3' and 5'-CCGTCTTTCATTACACAGGACA-3'; *Il6*, 5'-GAACAACGATGATGCACTTG-3' and 5'-CTTCATGTACTCCAGGTAGCTATGGT-3'; *Il10*, 5'-CAAGGAGCATTTGAATTCCC-3' and 5'-GGCCTTGTAGACACCTTGGTC-3'; *Il12a*, 5'-CGCAGCACTTCAGAATCACA-3' and 5'-TCTCCCACAGGAGGTTTCTG-3'; *Il12b*, 5'-GGAAGCACGGCAGCAGAATA-3' and 5'-AACTTGAGGGAGAAGTAGGAATGG-3'; *Ifng*, 5'-GACAATCAGGCCATCAGCAAC-3' and 5'-CGGATGAGCTCATTGAATGCTT-3'; *Tgfb1*, 5'-ATTCCTGGCGTTACCTTGG -3' and 5'-CCTGTATTCCGTCTCCTTGG-3'; *Nos2*, 5'-AGCCAAGCCCTCACCTACTT-3' and 5'-TCTCTGCCTATCCGTCTCGT-3'; *Arg1*, 5'-CAATGAAGAGCTGGCTGGTGT-3' and 5'-GTGTGAGCATCCACCCAAATG-3'; *Cd163*, 5'-GCAAAAACTGGCAGTGGG-3' and 5'-GTCAAAATCACAGACGGAGC-3'; *Mrc1*, 5'-TCTTTGCCTTTCCCAGTCTCC-3' and 5'-TGACACCCAGCGGAATTTC-3'. *Gapdh* (5'-GCCTTCCGTGTTCCTACCC-3' and 5'-CAGTGGGCCCTCAGATGC-3') was used as an internal standard. Amplification-curve plotting and calculation of ΔCt values were performed by a dedicated software.

Cytofluorimetric analysis

For FACS analysis, SeC monolayers were harvested, centrifuged (400g for 5 min) to form a cell pellet of approximately $1.0x10^6$ cells, and the supernatant was removed. The cells were fixed in 4% PFA in PBS for 30 min, washed in FACS buffer (PBS with 3% BSA), and treated with 0.1% Triton

X-100 in FACS buffer for 10 min. After centrifugation (400g for 5 min), the supernatant was removed, and the cells were blocked with 5 % BSA in FACS buffer for 1h at room temperature before incubation with primary antibody (AMH, INSL3, ASMA or PGP9.5, 1 µl antibody per 0.5-1.0x10^6 cells, or buffer alone) for 1h at room temperature. The cells were washed twice with 2 ml of FACS buffer per tube, pelleted by centrifugation (400g for 5 min), with the supernatant being removed. Lastly, the cells were exposed to the secondary Alexa 488-conjugated donkey anti-goat antibody (1:500) and Alexa 488-conjugated donkey anti-rabbit antibody (1:500) and suspended in 0.5 ml FACS buffer. Then, the cells were centrifuged (400g, 5 min), the supernatant was removed and pellet suspended again in 0.5 ml FACS buffer with 1% PFA for analysis. Data acquisition was performed on 1.0x10^4 events per tube based on a total (ungated) count of forward and side light scatter at approximately 200-300 events/sec on a BD FACSort flow cytometer and analyzed using FACS Diva software (both from BD Biosciences).

ELISA dosage

To quantitate the serum levels of heregulin β1 in SeC-MC- and mock-treated *mdx* mice, blood samples were collected one week after treatment, and the sera were analyzed by the ELISA kit for neuregulin 1 (isoform HRG-beta 1) (MBS913011, MyBioSource, USA) according to the manufacturer's instructions.

Functional evaluation

Functional recovery of skeletal muscles was evaluated by treadmill running tests performed after 3 weeks from the treatment. In treadmill endurance tests mice were first acclimated to the treadmill (LE 8710, PanLab, Spain) before running by placing them on an unmoving treadmill for 10 min. The treadmill was set at 0° inclination and 15 cm/sec speed. The test ran for 30 min, and the number of times at which mice failed to keep running was recorded. Each test was performed thrice a week during the third week of treatment, and the results were averaged for each mouse (n=10).

Exhaustion running tests were performed at day 21 post-injection. Mice were put into a 0° inclined treadmill (Columbus Instruments, USA) at 10 cm/sec, and the speed was increased by 5 cm/sec every 3 min until the mouse reached exhaustion, which was defined as a prolonged spending time (10 sec) on the shocker plate without attempting to reengage the treadmill. Total distance and running time were registered for each mouse (n=10).

Statistical analysis

Quantitative data are presented as means±SEM of at least three independent experiments. Representative experiments are shown unless stated otherwise. The data were subjected to analysis of variance (ANOVA) with SNK post-hoc analysis using a statistical software package (GraphPad Prism version 4.00, GraphPad).

References

1. Emery, A.E.H. 1993. Duchenne Muscular Dystrophy. Oxford University Press, ed. (Oxford, UK).
2. Blake, D.J., A. Weir, S.E. Newey, and K.E. Davies. 2002. Function and genetics of dystrophin and dystrophin-related proteins in muscle. *Physiol. Rev.* 82:291-329.
3. Porter, J.D., S. Khanna, H.J. Kaminski, J.S. Rao, A.P. Merriam, C.R. Richmonds, P. Leahy, J. Li, W. Guo, and F.H. Andrade. 2002. A chronic inflammatory response dominates the skeletal muscle molecular signature in dystrophin-deficient mdx mice. *Hum. Mol. Genet.* 11:263-272.
4. Evans, N.P., S.A. Misyak, J.L. Robertson, J. Bassaganya-Riera, and R.W. Grange. 2009. Immune mediated mechanisms potentially regulate the disease time course of Duchenne muscular dystrophy and provide targets for therapeutic intervention. *PM&R.* 1:755-768.

5. Khurana, T.S., and K.E. Davies. 2003. Pharmacological strategies for muscular dystrophy. *Nat. Rev. Drug Discov.* 2:379-390.

6. Goyenvalle, A., J.T. Seto, K.E. Davies, and J. Chamberlain. 2011. Therapeutic approaches to muscular dystrophy. *Hum. Mol. Genet.* 20:R69-R78.

7. Manzur, A.Y., T. Kuntzer, M. Pike, and A.V. Swan. 2008. Glucocorticoid corticosteroids for Duchenne muscular dystrophy. *Cochrane Database Syst. Rev.* 1:CD003725.

8. Skinner, M.K., and M.D. Griswold. 2005. *Sertoli Cell Biology*. Elsevier-Academic Press, San Diego, CA, USA.

9. Mital, P., G. Kaur, and J.M. Dufour. 2010. Immunoprotective Sertoli cells: making allogeneic and xenogeneic transplantation feasible. *Reproduction*. 139:495–504.

10. Sanberg, P.R., C.V. Borlongan, S. Saporta, and D.F. Cameron. 1996. Testis-derived Sertoli cells survive and provide localized immunoprotection for xenografts in rat brain. *Nat. Biotechnol.* 14:1692-1695.

11. Shamekh, R., N.S. El-Badri, S. Saporta, C. Pascual, P.R. Sanberg, and D.F. Cameron. 2006. Sertoli cells induce systemic donor-specific tolerance in xenogenic transplantation model. *Cell Transpl.* 15:45-53.

12. Sanberg, P.R., C.V. Borlongan, A.I. Othberg, S. Saporta, T.B. Freeman, and D.F. Cameron. 1997. Testis-derived Sertoli cells have a trophic effect on dopamine neurons and alleviate hemiparkinsonism in rats. *Nat. Med.* 3:1129-1132.

13. Rodriguez, A.I.A., E. Willing, S. Saporta, D.F. Cameron, P.R. Sanberg. 2003. Effects of Sertoli cell transplants in a 3-nitropropionic acid model of early Huntington's disease: a preliminary study. *Neurotox Res.* 5:443-450.

14. Hemendinger, R., J. Wang, S. Malik, R. Persinski, J. Copeland, D. Emerich, P. Gores, C. Halberstadt, and J. Rosenfeld. 2005. Sertoli cells improve survival of motor neurons in SOD1 transgenic mice, a model of amyotrophic lateral sclerosis. *Exp. Neurol.* 196:235-243.

15. Luca, G., M. Calvitti, C. Nastruzzi, L. Bilancetti, E. Becchetti, G. Angeletti, F. Mancuso, and R. Calafiore. 2007. Encapsulation, in vitro characterization, and in vivo biocompatibility of Sertoli cells in alginate-based microcapsules. *Tissue Eng.* 13:641-648.

16. Fallarino, F., G. Luca, M. Calvitti, F. Mancuso, C. Nastruzzi, M.C. Fioretti, U. Grohmann, E. Becchetti, A. Burgevin, R. Kratzer, P. van Endert, L. Boon, P. Puccetti, and R. Calafiore. 2009. Therapy of experimental type 1 diabetes by isolated Sertoli cell xenografts alone. *J. Exp. Med.* 206:2511-2526.

17. Luca, G., M. Calvitti, F. Mancuso, G. Falabella, I. Arato, C. Bellucci, E. O. List, E. Bellezza, G. Angeli, C. Lilli, M. Bodo, E. Becchetti, J.J. Kopchick, D.F. Cameron, T. Baroni, and R. Calafiore. 2013. Reversal of experimental Laron Syndrome by xenotransplantation of microencapsulated porcine Sertoli cells. *J. Control Release.* 165:75-81.

18. Cameron, D.F., J.J. Hushen, T. Dejarlais, L. Colado, K.M. Wolski, P.R. Sanberg, S. Saporta. 2002. A unique cytoplasmic marker for extratesticular Sertoli cells. *Cell Transplant.* 11:507-512.

19. Bistoni, G., M. Calvitti, F. Mancuso, I. Arato, G. Falabella, R. Cucchia, F. Fallarino, A. Becchetti, T. Baroni, S. Mazzitelli, C. Nastruzzi, M. Bodo, E. Becchetti, D.F. Cameron, G. Luca, and R. Calafiore. 2012. Prolongation of skin allograft survival in rats by the transplantation of microencapsulated xenogeneic neonatal porcine Sertoli cells. *Biomaterials.* 33:5333-5340.

20. Evans, N.P., S.A. Misyak, J.L. Robertson, J. Bassaganya-Riera, and R.W. Grange. 2009. Dysregulated intracellular signaling and inflammatory gene expression during initial disease onset in Duchenne muscular dystrophy. *Am. J. Phys. Med. Rehabil.* 88:502-522.

21. Ishizaki, M., T. Suga, E. Kimura, T. Shiota, R. Kawano, Y. Uchida, K. Uchino, S. Yamashita, Y. Maeda, and M. Uchino. 2008. Mdx respiratory impairment following fibrosis of the diaphragm. *Neuromuscul. Disord.* 18:342-348.

22. Villalta, S.A., C. Rinaldi, B. Deng, G. Liu, B. Fedor, and J.G. Tidball. 2011. Interleukin-10 reduces the pathology of mdx muscular dystrophy by deactivating M1 macrophages and modulating macrophage phenotype. *Hum. Mol. Genet.* 20:790-805.

23. Doyle, T.J., G. Kaur, S.M. Putrevu, E.L. Dyson, M. Dyson, W.T. McCunniff, M.R. Pasham, K.H. Kim, and J.M. Dufour. 2012. Immunoprotective properties of primary Sertoli cells in mice: potential functional pathways that confer immune privilege. *Biol. Reprod.* 86:1-14.

24. Bernasconi, P., E. Torchiana, P. Confalonieri, R. Brugnoni, R. Barresi, M. Mora, F. Cornelio, L. Morandi, and R. Mantegazza. 1995. Expression of transforming growth factor-beta 1 in dystrophic patient muscles correlates with fibrosis. Pathogenetic role of a fibrogenic cytokine. *J. Clin. Invest.* 96:1137-1144.

25. Villalta, S.A., H.X. Nguyen, B. Deng, T. Gotoh, and J.G. Tidball. 2009. Shifts in macrophage phenotypes and macrophage competition for arginine metabolism affect the severity of muscle pathology in muscular dystrophy. *Hum. Mol. Genet.* 18:482-496.

26. Perkins, K.J., and K.E. Davies. 2002. The role of utrophin in the potential therapy of Duchenne muscular dystrophy. *Neuromuscul. Disord.* 12:S78-S89.

27. Yamamoto, K., K. Yuasa, Y. Miyagoe, Y. Hosaka, K. Tsukita, H. Yamamoto, Y.I. Nabeshima, and S. Takeda 2000. Immune response to adenovirus-delivered antigens upregulates utrophin and results in mitigation of muscle pathology in mdx mice. *Hum. Gene Ther.* 11:669-680.

28. Pilgram, G.S., S. Potikanond, R.A. Baines, L.G. Fradkin, and J.N. Noordermeer. 2010. The roles of the dystrophin-associated glycoprotein complex at the synapse. *Mol. Neurobiol.* 41:1-21.

29. Gramolini, A.O., L.M. Angus, L. Schaeffer, E.A. Burton, J.M. Tinsley, K.E. Davies, J.P. Changeux, and B.J. Jasmin. 1999. Induction of utrophin gene expression by heregulin in skeletal muscle cells: role of the N-box motif and GA binding protein. *Proc. Natl. Acad. Sci. USA* 96:3223-3227.

30. Basu, U., M. Gyrd-Hansen, S.M. Baby, O. Lozynska, T.O. Krag, C.J. Jensen, M. Frödin, and T.S. Khurana. 2007. Heregulin-induced epigenetic regulation of the utrophin-A promoter. *FEBS Lett.* 581:4153-4158.

31. Krag, T.O., S. Bogdanovich, C.J. Jensen, M.D. Fischer, J. Hansen-Schwartz, E.H. Javazon, A.W. Flake, L. Edvinsson, and T.S. Khurana. 2004. Heregulin ameliorates the dystrophic phenotype in mdx mice. *Proc. Natl. Acad. Sci. USA.* 101:13856-13860.

32. Burks, T.N., Cohn, R.D. 2011. Role of TGF-β signaling in inherited and acquired myopathies. *Skelet. Muscle.* 1:19.

33. Stedman, H.H., H.L. Sweeney, J.B. Shrager, H.C. Maguire, R.A. Panettieri, B. Petrof, M. Narusawa, J.M. Leferovich, J.T. Sladky, and A.M. Kelly. 1991. The mdx mouse diaphragm reproduces the degenerative changes of Duchenne muscular dystrophy. *Nature.* 352:536-539.

34. Chiappalupi, S., Luca, G., Mancuso, F., Madaro, L., Fallarino, F., Nicoletti, C., Calvitti, M., Arato, I., Falabella, G., Salvadori, L., Di Meo, A., Bufalari, A., Giovagnoli, S., Calafiore, R., Donato, R. and Sorci, G. 2015. Effects of intraperitoneal injection of microencapsulated Sertoli cells on chronic and presymptomatic dystrophic mice. *Data in Brief*. Submitted.

35. Hunkeler, D., A.M. Sun, G.S. Korbutt, R.V. Rajotte, R.G. Gill, R. Calafiore, and P. Morel. 1999. Bioartificial organs and acceptable risk. *Nat Biotechnol.* 17:1045.

36. Calafiore, R., G. Basta, G. Luca, A. Lemmi, M.P. Montanucci, G. Calabrese, L. Racanicchi, F. Mancuso, and P. Brunetti, 2006. Microencapsulated pancreatic islet allografts into nonimmunosuppressed patients with type 1 diabetes: first two cases. *Diabetes Care.* 29:137-138.

37. Basta, G., P. Montanucci, G. Luca, C. Boselli, G. Noya, B. Barbaro, M. Qi, K.P. Kinzer, J. Oberholzer, and R. Calafiore. 2011. Long-term metabolic and immunological follow-up of nonimmunosuppressed patients with type 1 diabetes treated with microencapsulated islet allografts: four cases. *Diabetes Care.* 34, 2406-2409.

38. Godehardt, A.W., M. Rodrigues Costa, and R.R. Tönjes. 2015. Review on porcine endogenous retrovirus detection assays-impact on quality and safety of xenotransplants. *Xenotransplantation.* 22:95-101.

39. Arnold, L., Henry, A., Poron, F., Baba-Amer, Y., van Rooijen, N., Plonquet, A., Gherardi, R.K., and Chazaud, B. 2007. Inflammatory monocytes recruited after skeletal muscle injury switch into antiinfl ammatory macrophages to support myogenesis. *J. Exp. Med.* 204:1057-1069.

40. Ohlendieck, K., J.M. Ervasti, K. Matsumura, S.D. Kahl, C.J. Leveille, and K.P. Campbell. 1991. Dystrophin related protein is localized to neuromuscular junctions of adult skeletal muscle. *Neuron.* 7:499-508.

41. Clerk, A., G.E. Morris, V. Dubowitz, K. E. Davies, and C.A. Sewry. 1993. Dystrophin-related protein, utrophin, in normal and dystrophic human fetal skeletal muscle. *Histochem. J.* 25:554-561.

42. Helliwell, T.R., N.T. Man, G.E. Morris, and K.E. Davies. 1992. The dystrophin-related protein, utrophin, is expressed on the sarcolemma of regenerating human skeletal muscle fibres in dystrophies and inflammatory myopathies. *Neuromuscul. Disord.* 2:177-184.

43. Deutekom, J.C.T., and G.J.B. Ommen. 2003. Advances in Duchenne muscular dystrophy gene therapy. *Nat. Rev. Genet.* 4:774-783.

44. Tinsley, J., N. Deconinck, R. Fisher, D. Kahn, S. Phelps, J.M. Gillis, and K. Davies. 1998. Expression of full-length utrophin prevents muscular dystrophy in mdx mice. *Nat. Med.* 4:1441-1444.

45. Squire, S., J.M. Raymackers, C. Vandebrouck, A. Potter, J. Tinsley, R. Fisher, J.M. Gillis, and K.E. Davies. 2002. Prevention of pathology in mdx mice by expression of utrophin: analysis using an inducible transgenic expression system. *Hum. Mol. Genet.* 11:3333-3344.

46. Valdés-Gonzalez, R.A., D.J. White, L.M. Dorantes, L. Terán, G.N. Garibay-Nieto, E. Bracho-Blanchet, R. Dávila-Pérez, L. Evia-Viscarra, C.E. Ormsby, J.T. Ayala-Sumuano, M.L. Silva-Torres, and B. Ramírez-González. 2007. Three-yr follow-up of a type 1 diabetes mellitus patient with an islet xenotransplant. *Clin. Transpl.* 21:352-357.

47. Esquivel-Pérez, R., A.L. Rodriguez-Ventura, L.M. Dorantes, B. Ramírez-González, M.G. López-Santos, and R. Valdes-Gonzalez. 2011. Correlation between insulin requirements and

anti-galactose antibodies in patients with type 1 diabetes transplanted with neonatal pig islets. *Clin. Exp. Immunol.* 165:104-109.

48. Mather, J.P., and D.D. Philips. 1999. Primary culture of testicular somatic cells, in: Barnes, D.W., Sirbasku, D.A., and Sato, G.H. (Eds.), *Methods for Serum Free Culture of Cells of the Endocrine System*, New York Liss, New York, pp. 24-45.
49. Galdieri, M., E. Ziparo, F. Palombi, M.A. Russo, M.J. Stefanini. 1981. Pure Sertoli cell cultures: a new model for the study of somatic-germ cell interaction. *J. Androl.* 2:249–254.
50. Riuzzi, F., G. Sorci, R. Sagheddu, and R. Donato. 2012. HMGB1/RAGE regulates muscle satellite cell homeostasis via p38 MAPK/myogenin-dependent repression of Pax7 transcription. *J. Cell Sci.* 125:1440-1454.
51. Messina, S., Bitto, A., Aguennouz, M., Mazzeo, A., Migliorato, A., Polito, F., Irrera, N., Altavilla, D., Vita, G.L., Russo, M., Naro, A., De Pasquale, M.G., Rizzuto, E., Musarò, A., Squadrito, F., and Vita, G. 2009. Flavocoxid counteracts muscle necrosis and improves functional properties in mdx mice: a comparison study with methylprednisolone. *Exp. Neurol.* 220:349-358.

Acknowledgements

S.C. is recipient of a fellowship from the Regione Umbria, Italy (POR UMBRIA FSE 2007-2013). L.M. is recipient of an AFM (Association Française contre les Myopathies) fellowship. G.L. and R.C. were supported by a grant from Mr. Gary Harlem (Altucell, NY, USA). R.D. was supported by the AFM (Project 15679), the Ministero dell'Università e della Ricerca (PRIN 2010R8JK2X_004), and the Fondazione Cassa di Risparmio di Perugia (2009.020.0021 and 2012.0241.021). G.S. was supported by the Ministero dell'Università e della Ricerca (PRIN 2009WBFZYM_002). The funders had no role in study design, data collection and analysis, decision to publish, or preparation of the manuscript.

Author Contributions

S.C. co-designed the project, carried out the experimental work and analyzed the data. G.L. co-designed the project, led the Sertoli cells team which isolated SeC and injected SeC-MC, and interpreted the data. F.M., A.D.M. and A.B. performed orchidectomy in SPF Large White pigs, I.A. and G.F. purified and encapsulated porcine SeC, conducted experimental work and analyzed the data. S.G. evaluated barium release from microcapsules, L.M. and C.N. performed functional analyses. F.F. discussed the project and interpreted the data. M.C. performed SC isolation and histologic staining. L.S. carried out experimental work. R.C. and R.D. supervised the research and edited the manuscript. G.S. co-designed the project, supervised the research and wrote the manuscript. All authors discussed the data and the manuscript.

Figure legends

Figure 1. SPF SeC-MC show homogeneous morphology, and high retention of cell viability and functional integrity of encapsulated cells. (A,B) Isolated SPF SeC were characterized for the expression of anti-Müllerian hormone (AMH), insulin-like 3 (INSL3), α-smooth muscle actin (ASMA), and protein gene product 9.5 (PGP9.5) by FACS analysis (A) and immunofluorescence staining (*green*) (B). Nuclei were counterstained with DAPI (*blue*). The percentages of positive SeC for each antigen (n=5) (A,B) are indicated. **(C)** Representative images of empty microcapsules (E-MC) and microcapsules containing SPF SeC (SeC-MC) as observed by bright field microscopy. **(D)** The viability of isolated SFP SeC was evaluated before and after encapsulation by ethidium bromide (*orange*) and fluorescein diacetate (*green*) double staining. Reported are representative images with indicated the average percentages of viable cells (means±SEM) of three different experiments. **(E)** α-Aromatase activity expressed in terms of 17-β-estradiol biosynthesis per $1.0x10^6$

cells was determined in the absence or presence of folliculostimulating hormone (FSH) in free (monolayer) and microencapsulated SeC (SeC-MC). *, significantly different from control ($p \leq 0.001$).

Figure 2. A single i.p. injection of SeC-MC improves muscle morphology in *mdx* mice. Freshly prepared SeC-MC or E-MC were injected into the peritoneal cavity of 4-week-old *mdx* mice. Muscles from mock-treated (n=8) and SeC-MC-treated (n=8) mice were analyzed three weeks after injection. **(A-C)** TA muscle morphology was evaluated after haematoxylin/eosin staining (A). The mean percentages (±SEM) of undamaged, regenerating, regenerated, and necrotic myofibers (B), and the cross-sectional area (CSA) of myofibers (C) were determined. The mean CSA (μm^2) for mock- and SeC-MC-treated mice is reported (box in C). **(D,E)** Infiltrating macrophages were detected using an anti-MAC3 antibody (*brown*). Reported are representative images of TA muscle (D). The mean percentages (±SEM) of $MAC3^+$ areas in TA, GC and DIA were determined (E). **(F,G)** Mallory staining shows reduced fibrous tissue (*blue*) infiltration in TA of SeC-MC-treated compared with mock-treated *mdx* mice (F). The mean percentages (±SEM) of fibrotic areas in TA, GC and DIA were determined (G). *, significantly different from control ($p \leq 0.001$). Original magnification (A,D,F), 20x.

Figure 3. SeC-MC-treated *mdx* mice show recovery of muscle performance. (A) Four-week-old *mdx* mice i.p. injected with SeC-MC (n=10) or empty microcapsules (Mock; n=10) were evaluated for muscle performance in treadmill exercise tests. These were performed every two days for a total of five times starting at week 3 post-injection. Age-matched untreated WT (C57Bl/10) mice (n=10) were tested in parallel. Reported are the average numbers (±SEM) of stops recorded from mice of each group during a 30-min running on the fifth running day. **(B)** Four-week-old *mdx* mice treated as in (A) (each group n=10) were evaluated for muscle performance by exhaustion running test. Reported are the covered distances (*left panel*) and times to exhaustion (*right panel*) in comparison

with age-matched untreated WT mice (n=10). **(C,D)** After the last running mice in *a* were i.p. injected with Evans Blue Dye (EBD) and after an additional 24h TA, GC and QF muscles were isolated (C) and cryosectioned for detection of EBD infiltration (*red*). Shown in (D) are representative images of QF in which individual muscle fibers were delineated with laminin staining (*green*), and nuclei were counterstained with DAPI (*blue*). Reported are the average percentages (±SEM) of EBD-positive myofibers in each group (D). * and #, significantly different from WT control ($p \leq 0.005$) and mock-treated *mdx* ($p \leq 0.005$) mice, respectively. Original magnification (D), 20x.

Figure 4. The antiinflammatory effects of SeC-MC are evident even one week after injection. (A,B) One week after injection TA muscles from mock-treated (n=5) and SeC-MC-treated (n=6) 4-week-old *mdx* mice were analyzed for the presence of $MAC3^+$ cells by immunohistochemistry (A, *arrows*) or the expression of MAC3 by Western blotting (B). The mean percentages (±SEM) of $MAC3^+$ areas (A) and the average relative densities of MAC3 bands with respect to GAPDH bands (B) were determined. **(C,E)** One week after injection lympho-mononuclear cell infiltrate from hind limb muscles of mock-treated (n=6) and SeC-MC-treated (n=6) 4-week-old *mdx* mice were analyzed by real-time PCR for the expression of the indicated cytokines (C), inducible nitric oxide (*Nos2*) and arginase 1 (*Arg1*) (D), and CD163 (*Cd163*) and CD206 (*Mrc1*) (E). Reported are the values of percent increments (±SEM) with respect to mock-treated mice (C,E). Original magnification (A), 40x. * and **, significantly different from mock-treated control at $p \leq 0.001$ and $p \leq 0.01$, respectively.

Figure 5. Muscles from SeC-MC-treated *mdx* mice show heregulin β1-induced expression of utrophin at the myofiber periphery. (A-C) One week after injection hind limb muscles from 4-week-old *mdx* mice i.p. injected with SeC-MC (n=6) or empty microcapsules (Mock; n=5) were analyzed by real-time PCR (A) or Western blotting (B) for utrophin (*Utrn*) expression. The average

relative densities (±SEM) of utrophin bands relative to α-actinin bands were determined (B). Immunofluorescence analysis of utrophin in myofibers of TA muscles of SeC-MC-treated *mdx* mice is shown in (C). **(D)** Western blot analysis of heregulin β1 in encapsulated porcine SeC (SeC-MC) conditioned medium. Empty microcapsules were used as a control (−). **(E)** ELISA dosage of serum levels (ng/ml) of heregulin β1 in SeC-MC-treated (n=10) and mock-treated (n=8) 4-week-old *mdx* mice one week after injection. **(F-I)** SeC-MC-treated 4-week-old *mdx* mice were i.p. injected with anti-heregulin β1 antibody (0.5 mg/kg body weight) (n=6) or the same amount of non-immune IgG (n=6) every other day for one week starting from the day of injection. Mice injected with empty microcapsules and treated with non-immune IgG (Mock; n=5) were used as a control. The relative amounts of utrophin in the TA muscles were determined by Western blotting (F). The average relative densities (±SEM) of utrophin bands with respect to α-actinin bands were determined (F). Formalin-fixed paraffin-embedded TA muscles were analyzed in H&E or immunohistochemistry for the presence of $MAC3^+$ cells (macrophages), and fresh-frozen TA muscles were analyzed by immunofluorescence for utrophin expression (G). Reported are the mean percentages of necrotic myofibers (H), and $MAC3^+$ areas (I). * and **, significantly different from mock-treated control at $p \leq 0.001$ and $p \leq 0.01$, respectively. #, significantly different from internal control (IgG-injected SeC-MC-treated mice) ($p \leq 0.001$). Original magnification (C; G, *middle lane*), 40x; (G, *upper and lower lanes*), 20x.

Figure 6. A single i.p. injection of SeC-MC preserves muscle homeostasis in long-term treatment in *mdx* mice. (A,B) Five months after i.p. injection into 4-week-old *mdx* mice (n=10 each group), empty microcapsules (E-MC) (A) and SeC-MC (B) were recovered from the peritoneal cavity and analyzed by phase contrast microscopy. **(C)** Viability of SeC inside the microcapsules was analyzed by ethidium bromide (*orange*)/fluorescein diacetate (*green*) staining. Indicated is the average percentage (±SEM) of viable cells. **(D-F)** Five months after injection, 4-week-old *mdx* mice

treated with SeC-MC (n=5) or E-MC (Mock) (n=5) were i.p. injected with EBD 24h before being sacrificed. DIA were isolated (D), cryosectioned and analyzed for EBD infiltration (*red*) (E,F). Cryosections were treated with an anti-laminin antibody (*green*) to mark individual myofibers, and nuclei were counterstained with DAPI (*blue*). The average percentage (±SEM) of EBD-positive (damaged) myofibers in each group is indicated. **(G-O)** DIA from 4-week-old *mdx* mice injected with SeC-MC (n=6) or empty microcapsules (Mock) (n=6) were analyzed five months later by H&E (G,H) or Mallory (I,J) staining, and immunohistochemistry for MAC3 (K,L) or immunofluorescence on frozen sections for utrophin (M,N) expression. Arrow (G) and arrowhead (K) in mock-treated DIA point to adipose tissue and inflammatory cells infiltrate, respectively. The average percentages (±SEM) of fat deposition (G,H), and fibrotic (I,J) and $MAC3^+$ (K,L) areas in mock- and SeC-MC-treated DIA are shown (O). *, significantly different from control ($p \leq 0.001$). Bars (A-C), 200 µm. Original magnification (E,F,I-L), 20x; (G,H), 10x; (M,N), 40x.

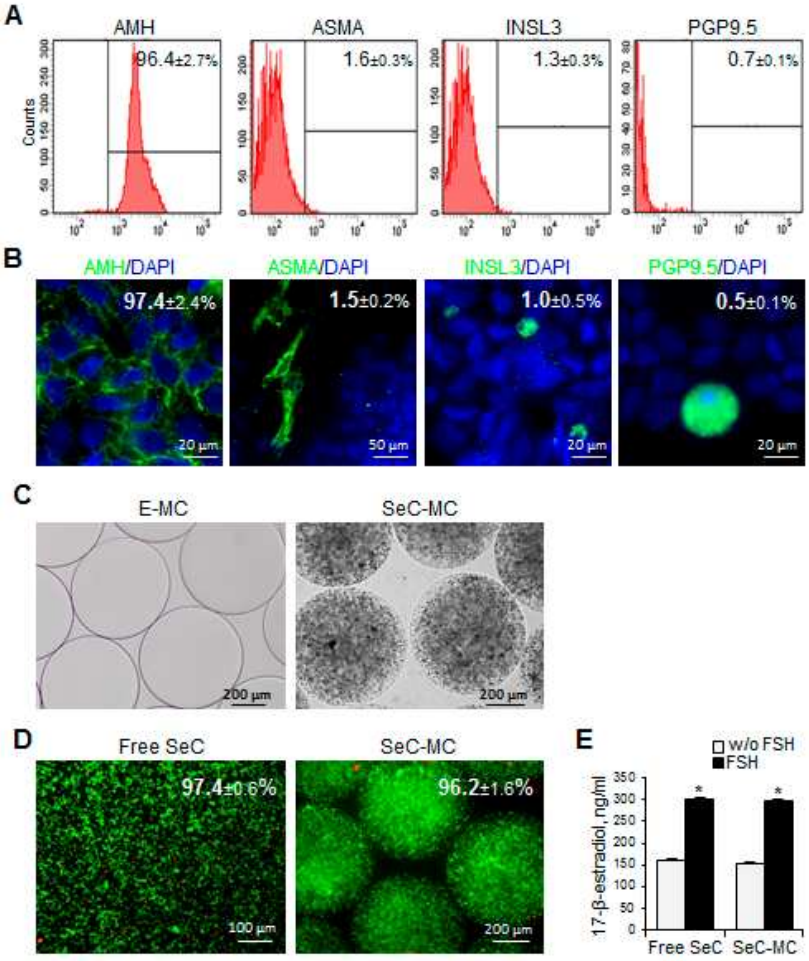

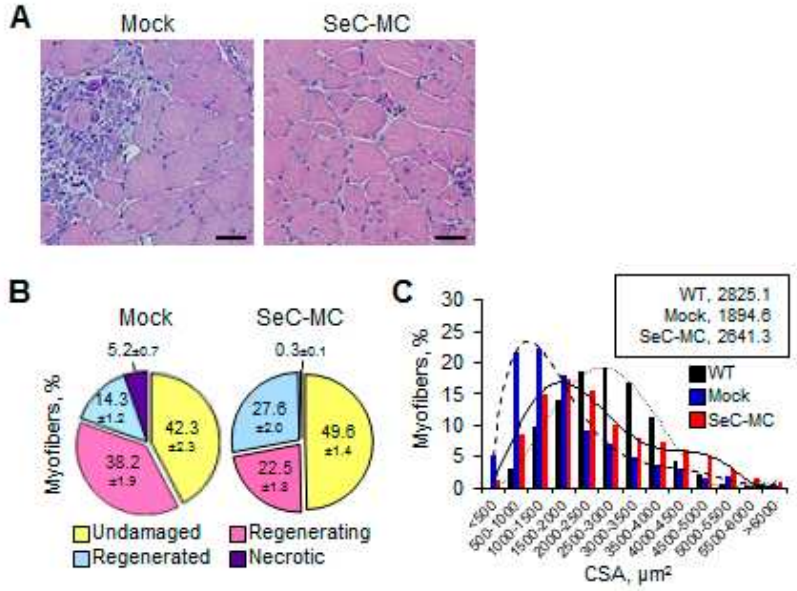
A
Mock
SeC-MC
B
Mock
SeC-MC
5.2±0.7
0.3±0.1
14.3 ±1.2
42.3 ±2.3
38.2 ±1.9
27.6 ±2.0
22.5 ±1.8
49.6 ±1.4
Myofibers, %
Undamaged
Regenerated
Regenerating
Necrotic
C
WT, 2825.1
Mock, 1894.6
SeC-MC, 2641.3
WT
Mock
SeC-MC
Myofibers, %
CSA, µm²
D
Mock
SeC-MC
E
Mock
SeC-MC
MAC3⁺ area, %
TA
GC
DIA
F
Mock
SeC-MC
G
Mock
SeC-MC
Fibrotic area, %
TA
GC
DIA

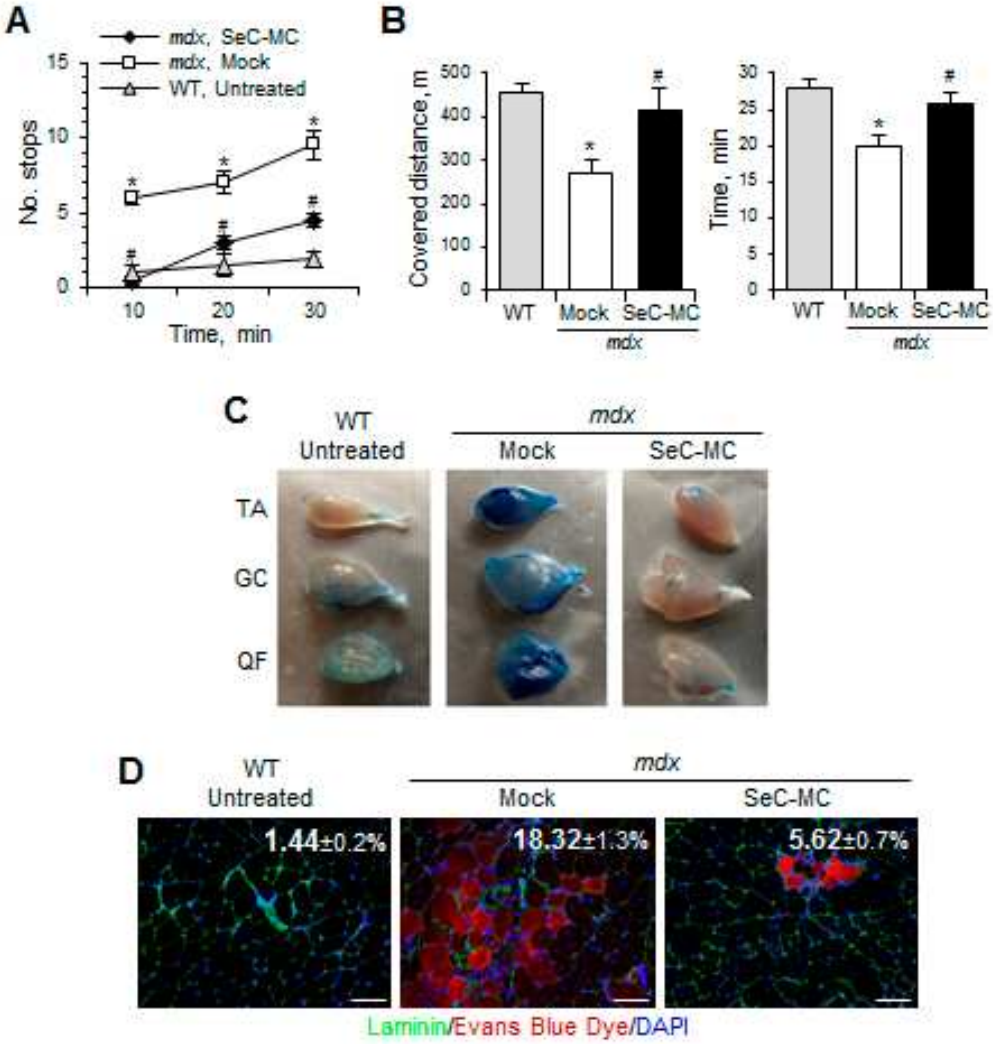

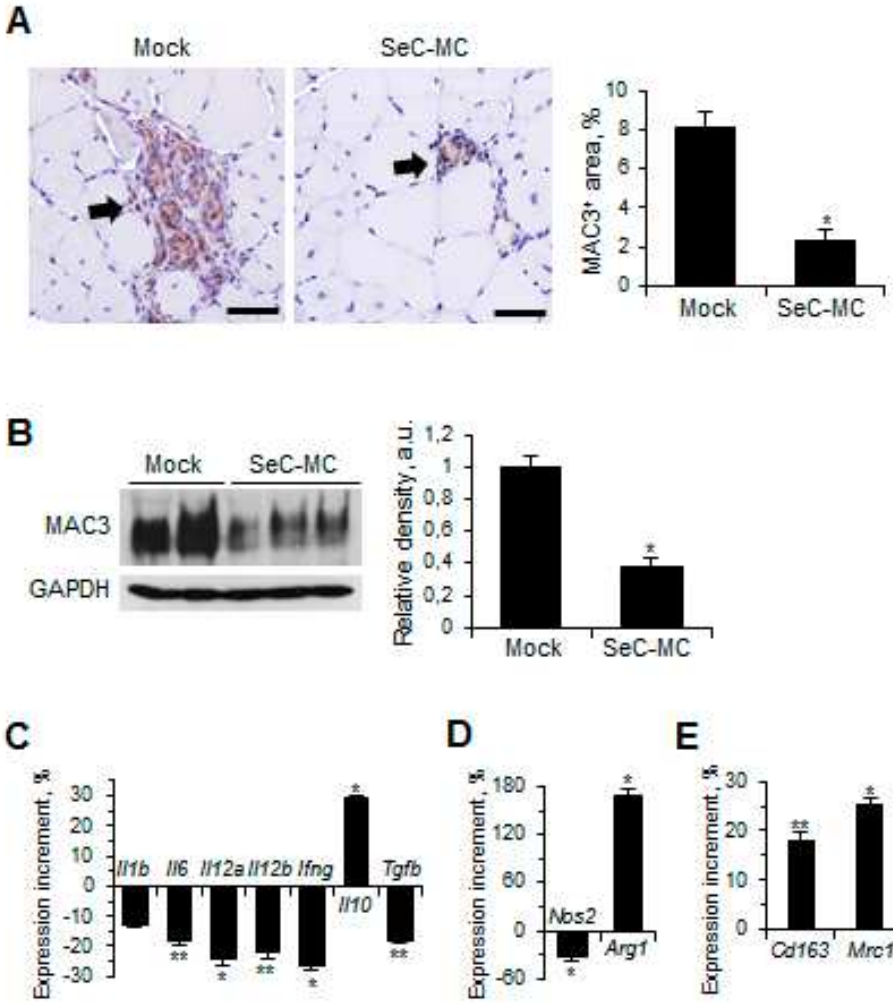

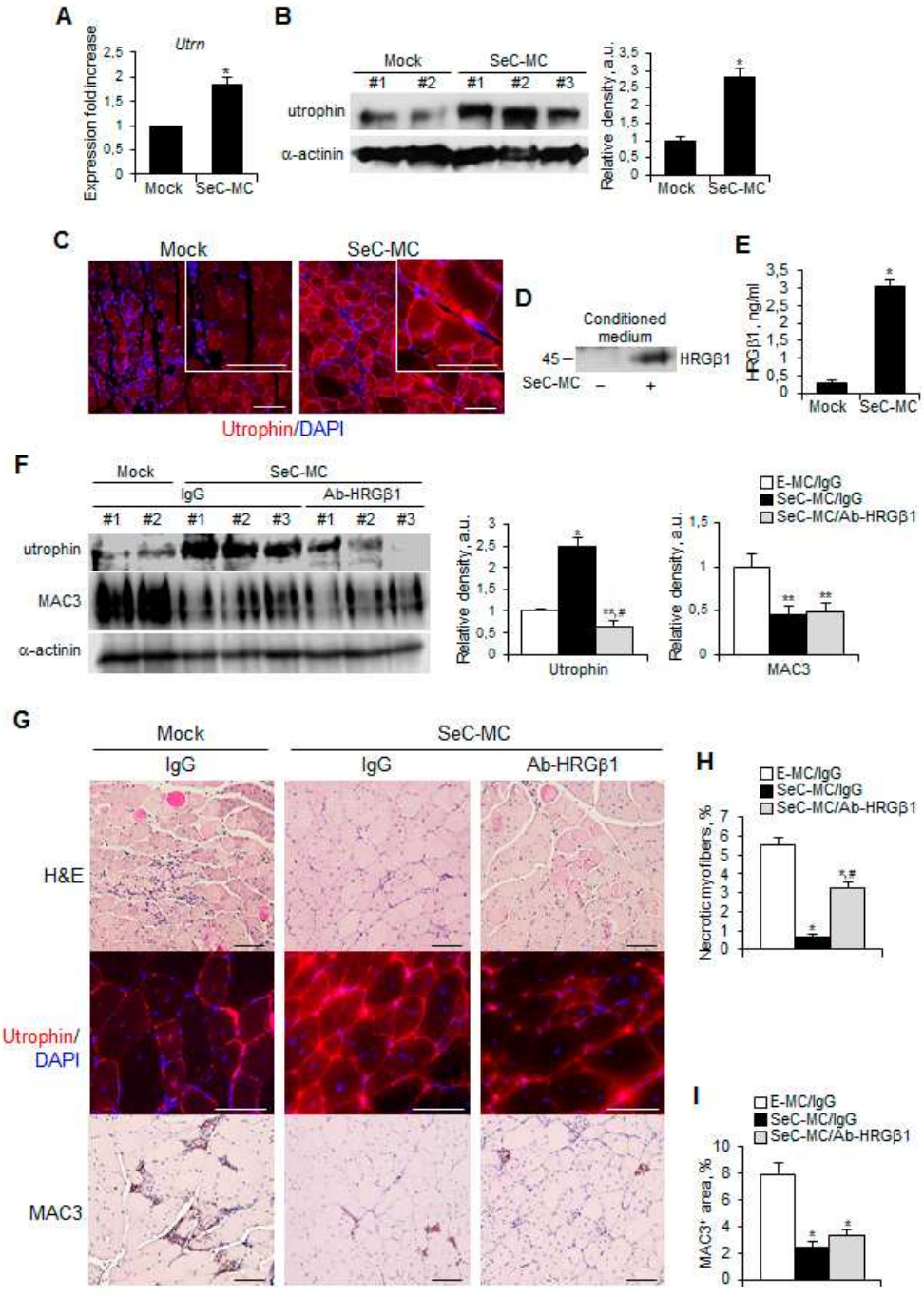
A
Utrn
Expression fold increase
Mock
SeC-MC
B
Mock
SeC-MC
#1 #2 #1 #2 #3
utrophin
α-actinin
Relative density, a.u.
C
Mock
SeC-MC
Utrophin/DAPI
D
Conditioned medium
45
HRGβ1
SeC-MC – +
E
HRGβ1, ng/ml
F
Mock
SeC-MC
IgG
Ab-HRGβ1
utrophin
MAC3
α-actinin
E-MC/IgG
SeC-MC/IgG
SeC-MC/Ab-HRGβ1
Utrophin
MAC3
G
H&E
Utrophin/ DAPI
MAC3
H
Necrotic myofibers, %
I
MAC3+ area, %

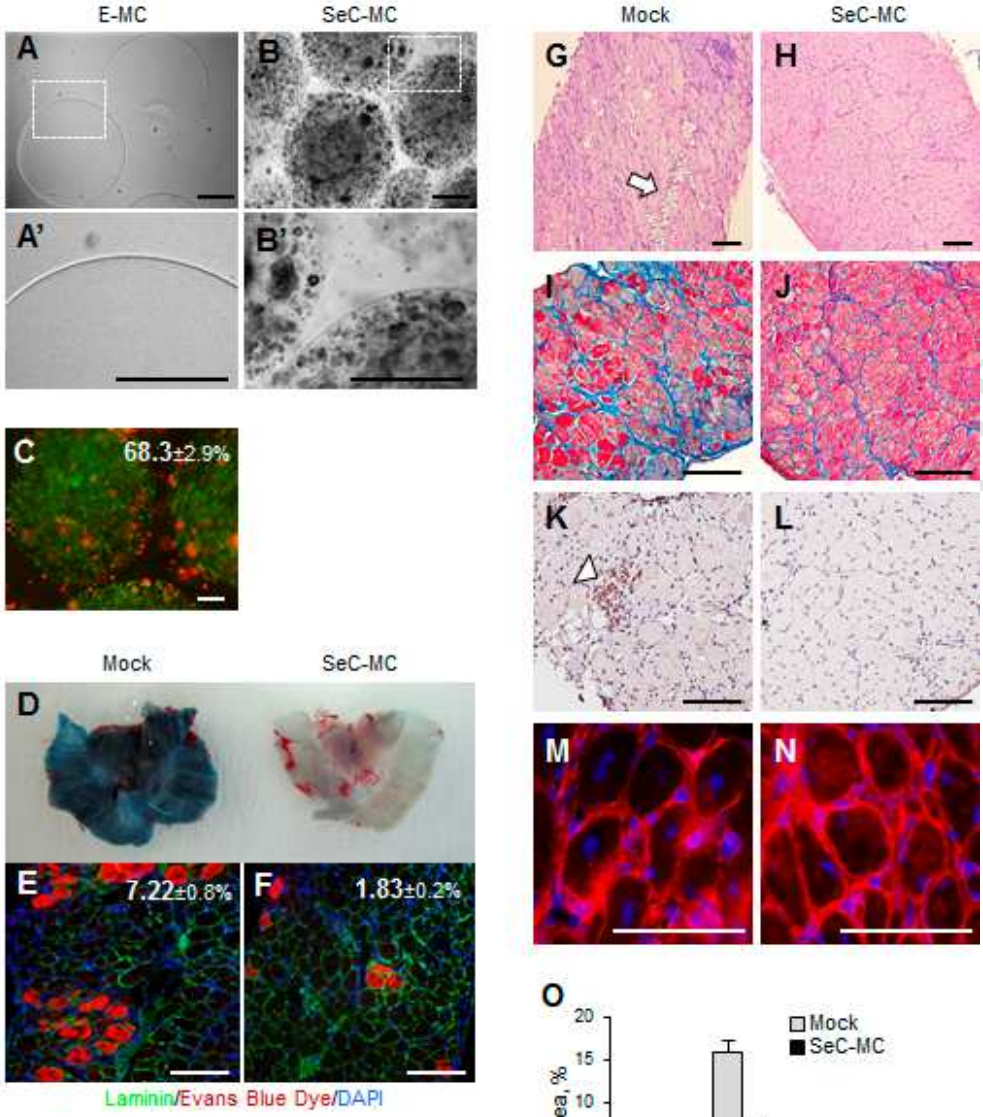
E-MC
SeC-MC
A
B
A'
B'
C
68.3±2.9%
Mock
SeC-MC
D
E
7.22±0.8%
F
1.83±0.2%
Laminin/Evans Blue Dye/DAPI
Mock
SeC-MC
G
H
I
J
K
L
M
N
O
Mock
SeC-MC
Area, %
20
15
10
5
0
Adipose
Fibrotic
MAC3+